

Haptic Discrimination of Softness in Teleoperation: The Role of the Contact Area Spread Rate

Antonio Bicchi, Enzo Pasquale Scilingo, Danilo De Rossi

Keywords— Haptic sensors, Haptic displays, Teleoperation, Remote Palpation, Minimally-Invasive Surgery.

Abstract— Many applications in teleoperation and virtual reality call for the implementation of effective means of displaying to the human operator information on the softness and other mechanical properties of objects being touched. The ability of humans to detect softness of different objects by tactual exploration is intimately related to both kinesthetic and cutaneous perception, and haptic displays should be designed so as to address such multimodal perceptual channel. Unfortunately, accurate detection and replication of cutaneous information in all its details appears to be a formidable task for current technology, causing most of today's haptic displays to merely address the kinesthetic part of haptic information. In this paper we investigate the possibility of surrogating detailed tactile information for softness discrimination, with information on the rate of spread of the contact area between the finger and the specimen as the contact force increases. Devices for implementing such a perceptual channel are described, and a practical application to a mini-invasive surgery tool is presented. Psychophysical test results are reported, validating the effectiveness and practicality of the proposed approach.

I. INTRODUCTION

When exploring such mechanical properties of an object as stiffness, damping, hysteresis, etc., humans use their fingers to squeeze or indent the surfaces, and gather data from many sensory receptors in the hand. The variety of sensors used in such tasks can be divided in two broad functional classes, or sensory channels, namely kinesthetic and tactile (cutaneous or subcutaneous) sensors (see e.g. [10]). Kinesthetic information refers to geometric, kinetic and force data of the limbs, such as position and velocity of joints, actuation forces, etc., which is mainly mediated by sensory receptors in the muscles, articular capsulae, and tendons. Cutaneous information refers to pressure and indentation distributions, both in space (on the skin) and in time, and is mediated by mechanoreceptors innervating the derma and epidermis of the fingerpads. Other sensory information (such as thermal) may also be relevant to exploration by touch. Information synergistically conveyed by the kinesthetic and tactile channels, and elicited by the central nervous systems, forms the object of “haptic”, or touch-related, sciences and technologies [14].

In this paper, we focus our attention on a particularly important and interesting haptic task, i.e. discrimination of different objects by their compliance¹, and on the real-

A. Bicchi is with the Interdept. Research Center “E. Piaggio”, University of Pisa, Italy and the Dept. of Electrical Systems and Automation, University of Pisa, Italy. E-mail: bicchi@ing.unipi.it

E. P. Scilingo is with Interdept. Research Center “E. Piaggio”, University of Pisa, Italy. E-mail: pasquale@piaggio.cci.unipi.it

D. De Rossi is with Interdept. Research Center “E. Piaggio”, University of Pisa, Italy and the of C.N.R. Inst. Fisiologia Clinica, Pisa, Italy. E-mail: derossi@piaggio.cci.unipi.it

¹What in common language is referred to as discrimination by com-

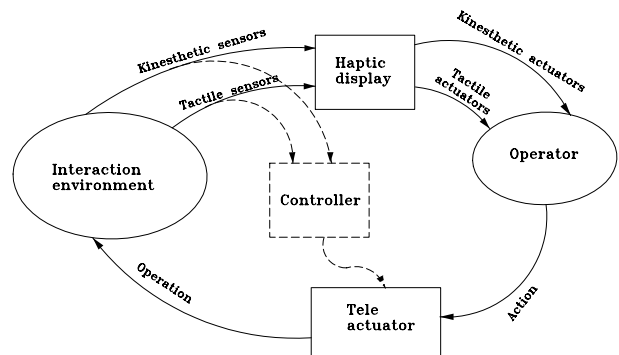


Fig. 1. A schematic representation of a Remote Haptic System. At a conceptual level, haptic information is comprised of kinesthetic and tactile information. The scheme does not necessarily imply that different hardware should be used to implement the two channels.

ization of a system for allowing an operator to remotely perform such operation, i.e. a Remote Haptic System. An RHS is comprised in general of a *telemanipulator*, allowing the human operator to perform exploratory actions on the remote specimen, and a *haptic perceptual channel*, conveying back information to the operator (see fig.1). Communication of haptic information involves both sensing performed at the remote end of the loop, and display on the operator side. In full generality, both kinesthetic and tactile information should be sensed at one end, and displayed at the other end.

As a matter of fact, at the present state of the art and technology most RHS only implement the kinesthetic channel. Indeed, the parts of a haptic system that refer to cutaneous tactile information are the most difficult to realize. Although there have been prototypal implementations of such sensory and displaying systems, such as e.g. those described by [7] and [9], the need for miniaturization, simplicity, economy, and ruggedness of many applications, makes the display of tactile information indeed a formidable task. On the other hand, the tactile component of haptics is by no means of secondary importance. In fact, in the psychophysical literature, it has been firmly established by the fundamental work of [21] and [12] that loss of the tactile channel reduces human capability of haptic discrimination dramatically.

To illustrate a particular, but important example of a RHS, let us refer to the case of a system for remote palpation of tissues in minimally invasive laparoscopy. This application, which has been considered by several authors

pliance may actually involve the object's perceived stiffness as well as damping, plasticity, hysteresis, etc., i.e., more precisely, its rheology.

([6], [9], [5], [2]), is one of the most promising for the new haptic technologies. As reported elsewhere ([20], [2]), imperfections and mechanical disadvantage in conventional forceps may substantially impair the surgeon's capability of tissue discrimination by palpation. This is particularly unfortunate in operations where camera information alone is not sufficient (for instance, nodular lesions of the lung have the same visual appearance as normal pulmonary tissue). To replace the missing haptic information, devices can be designed that implement, at least partially, the loop drawn in fig.1 (here, the "telem manipulator" is quite simply embodied by the standard laparoscopic tool handled by the surgeon). Purely kinesthetic sensors and devices can be implemented rather easily for this application (see e.g. devices described in [15] or [19]). On the contrary, tactile sensing should be implemented right on the small tips of the forceps jaws in the form of an array of distributed pressure-sensitive elements, with the relative harnessing problems; and tactile actuation should be realized by an array of micro-mechanical indenters, acting on the operator fingerpad. Although possible, such realizations may result too costly and not robust enough for large volume applications.

In this paper, we consider the problem of simplifying tactile sensors and displays to an extent which may represent a realistic tradeoff between what is needed perceptually and what can be provided technologically. More specifically, we illustrate a psychophysical hypothesis concerning a much simplified form of tactile information, which we call the Contact Area Spread Rate (CASR) paradigm. Devices for sensing and displaying the CASR are presented, and experiments are reported that validate, albeit preliminarily, the CASR paradigm as a viable approach to a complete haptic system.

II. THE CASR HYPOTHESIS.

As already stated, artificially reproducing tactile information in a manner which is comparable to what is naturally sensed is probably not feasible at the time being. However, tactile information in humans is extremely rich in content and purposes, and it might not be the case that all its richness is actually necessary to discriminate softness of different materials, which is our ultimate goal in this research. As an example, it seems a rather obvious observation that, up to some undesirable "haptic illusions", softness discrimination is not affected by the finger touching the surface of a specimen at different orientations; nor is it very sensitive to the location of the contact area on the finger surface. Such observations lead one to consider haptic discrimination of softness as fundamentally invariant with translations and rotations of the contact area.

One may go further on this line of reasoning, and conjecture other aspects of fine cutaneous imaging available to humans, to be scarcely relevant to haptic discrimination of softness. For instance, at least at the intuitive level, it might be suggested that the actual *shape* of the contact zone between the finger and the object is not as relevant to discrimination by compliance as the *area* of the zone itself.

More precisely, we *conjecture* that a large part of haptic

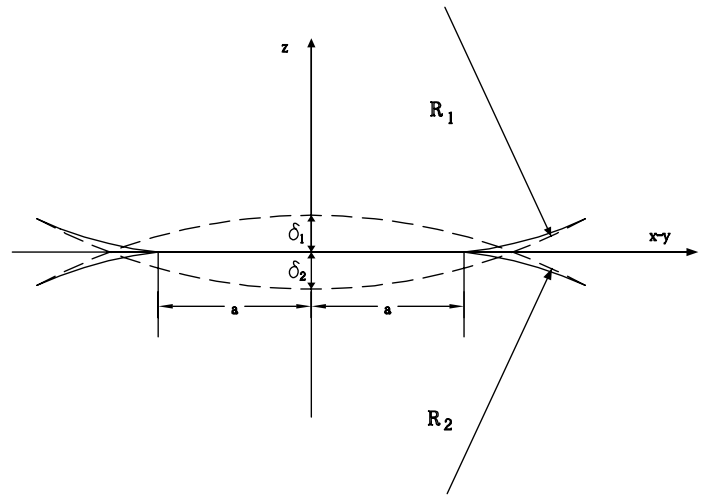


Fig. 2. Hertzian contact between two bodies.

information necessary to discriminate softness of objects by touch is contained in the law that relates resultant contact force to the overall area of contact, or in other terms in the rate by which the contact area spreads over the finger surface as the finger is increasingly pressed on the object. We call this relationship the Contact Area Spread Rate (CASR).

Clearly, such a conjecture does not imply that all other aspects of tactile information (such as e.g. the shape of the contact zone or the pressure distribution in the contact area) are not relevant to the task: rather, it suggests that, in the lack of better resources, the CASR information might be an acceptable surrogate for the complete sense of touch.

As a further motivation for such a hypothesis, consider standard Hertz modeling of contact between elastic bodies [11]. Although this theory applies to homogeneous, isotropic bodies of size much larger than that of the contact area, and this is not usually the case in many RHS applications (such as e.g. in laparoscopic surgery), still it is interesting to verify that our hypothesis makes sense in this case².

In the hertzian contact between two spheres, the contact area has circular shape of radius a , and the equation describing the relative displacement of corresponding points of objects within the contact area is

$$\bar{u}_{z1} + \bar{u}_{z2} = \delta - \frac{r^2}{2R} \quad (1)$$

where $\delta = \delta_1 + \delta_2$ is the relative displacement of two bodies, $\frac{1}{R} = \frac{1}{R_1} + \frac{1}{R_2}$ is the relative curvature, r is the radial distance from the center of contact ($r \leq a$) (see fig.2).

The pressure distribution law proposed by Hertz is given by

$$p(r) = p_0 \left[1 - \left(\frac{r}{a} \right)^2 \right]^{\frac{1}{2}}, \quad (2)$$

²a similar extrapolation of Hertz theory of contact has been used in [18] to set the reference deformation profile for an array of controlled pins on a distributed tactile display

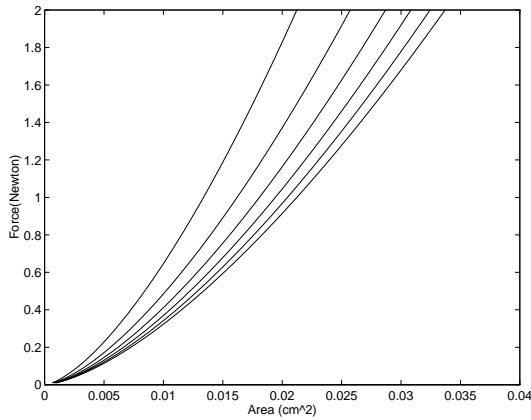


Fig. 3. Contact force/area curves for the hertzian model of contact between a spherical finger with $E_1 = 0.25MPa$, $\nu_1 = 0.5$, $R_1 = 5mm$, and six specimens with $\nu_2 = 0.5$, $R_2 = 10mm$, and E_2 ranging linearly between $E_1/2$ and $2E_1$.

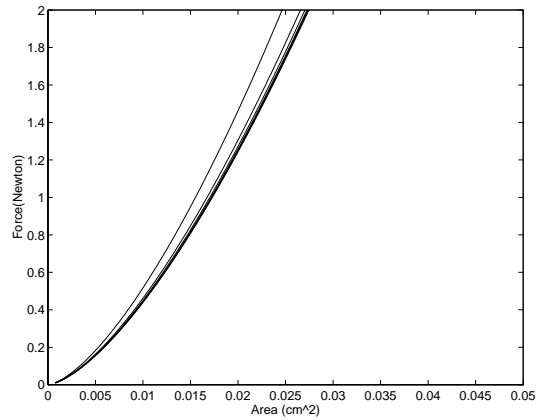


Fig. 4. Contact force/area curves for the hertzian model of contact between a finger as above, and six specimens with $\nu_2 = 0.5$, $E_2 = 0.125MPa$, and R_2 ranging linearly between $5R_1$ and $50R_1$.

and the displacements within the loaded area are

$$\bar{u}_{zi} = \frac{1 - \nu_i^2}{E_i} \frac{\pi p_0}{4a} (2a^2 - r^2), \quad r \leq a. \quad (3)$$

By substituting the expressions for \bar{u}_{z1} and \bar{u}_{z2} in equation 1 we get

$$\frac{\pi p_0}{4aE^*} (2a^2 - r^2) = \delta - \frac{r^2}{2R}. \quad (4)$$

where $\frac{1}{E^*} = \frac{1 - \nu_1^2}{E_1} + \frac{1 - \nu_2^2}{E_2}$, and E_i denotes the Young's modulus of the i -th body. From Eq. 4 the radius of the contact circle is obtained as

$$a = \frac{\pi p_0 R}{2E^*}. \quad (5)$$

The total force compressing the bodies being related to pressure by

$$F = \int_0^a p(r) 2\pi r dr = \frac{2}{3} p_0 \pi a^2, \quad (6)$$

using equation 5 we can relate the area of the contact disk A to force F as

$$A = \pi a^2 = \pi \left(\frac{3FR}{4E^*} \right)^{\frac{2}{3}}. \quad (7)$$

Contact between a “finger” with given elastic and geometric parameters E_1, ν_1, R_1 and “specimens” with varying elastic coefficients yield different rates of spread of the contact area A with the contact force F , as illustrated in fig.3. The CASR obtained from equation 7 depends also from the geometry of the specimens. However, in the range of geometric and elastic parameters that are relevant to our touch problem (ranges are described in fig.3 and fig.4), dependence on geometry is weaker than that on the elastic coefficient. This is especially evident for specimens larger than the probing finger (see fig.4).

III. IMPLEMENTATION OF CASR SENSORS AND DISPLAYS

In order for the CASR hypothesis to be of practical value in remote haptic system design, two main ingredients are necessary: a psychophysical validation, and a practical implementation of sensors and actuators that could convey the CASR information. It should be noticed that CASR information is basically comprised of two time signals (force and area of contact) of analogic nature: this is to be contrasted with tactile information, where a time-varying spatial distribution of pressures need to be sampled in both time and space. Thus, at least in principle, sensing and actuation of CASR information should be much easier and faster. In this section, we describe very simple devices that may be implemented for realizing CASR transduction, which are used later for validation experiments.

A. CASR sensors

A first type of CASR sensor can be built using piezoelectric or piezoresistive materials. In both cases, a thin film of the material is covered with two conductive layers on opposite sides (see fig.5), and an electric signal (the electric charge or the resistance, respectively) is measured by suitable instrumentation (a charge amplifier or a Wheatstone bridge and differential amplifier, respectively). The charge displaced per unit area on the electrodes is related to mechanical pressure as $q = \alpha p^\phi$, where α and ϕ are characteristic constants of the material ($\phi = 1$ in the ideal linear case). Assuming uniform pressure distribution, the total charge on the electrodes is $Q = \int q dA = \alpha p^\phi A$. An independent measurement of the total contact force $F = \int p dA = pA$ allows to derive a measure of the contact area as $A = \left(\frac{Q}{\alpha F^\phi} \right)^{\frac{1}{1-\phi}}$, hence to characterize the CASR curve. Analogously, in the piezoresistive case, the unit area of the conductive rubber layer changes its resistance according to $r = \beta p^{-\psi}$, and, in the uniform pressure distribution assumption, one gets $A = \left(\frac{\beta}{RF^\psi} \right)^{\frac{1}{1-\psi}}$, where

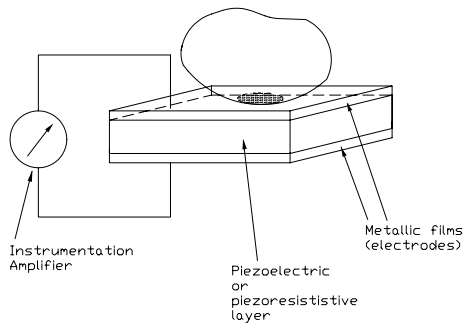


Fig. 5. Schematic drawing of a piezoelectric or piezoresistive CASR sensor.

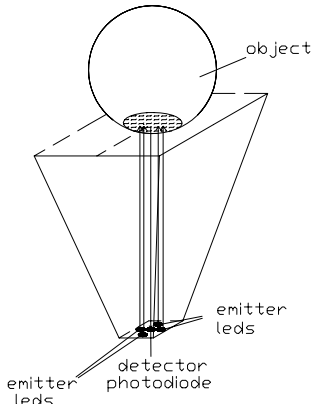


Fig. 6. The optoelectronic CASR sensor used in our experiments.

$R = \int r dA = \beta p^\psi A$ is the measured resistance. These formulas are to be considered as rough approximations of the real behaviour of sensors, where many effects (such as nonuniform pressure and shear effects) may be practically relevant (of the order of 10% or more, [17]). In practice, experimental calibration of sensors would be necessary to obtain a tabulated CASR response. The above approaches to CASR sensing have the advantage of an extremely simple implementation, allowing for instance the realization of a contact area sensor on the tips of a laparoscopic forceps with the need of a single wire to convey the signal (in this case, the force measurement could be provided e.g. by strain-gauges that are already available in some instrumented tools, see e.g. [2]). The material used in the piezoelectric or resistive layer should be prepared so as to enhance its nonlinearity: the sensitivity of these sensors tends to zero as ϕ (resp., ψ), tends to unity.

Another approach to CASR sensing that directly measures the contact area would use optoelectronic components to remotely measure changes in illumination due to changes of contact area. An example of optoelectronic CASR sensor is described in fig.6. The surface of the probing finger is realized with a transparent material (Plexiglas), and a LED/phototransistor pair is placed beneath the surface at a distance of few millimeters. The infrared LED emission is scattered over a wide cone, and is partially reflected at the interface of the finger with the outer environment. Reflection is negligible at points of the finger surface not



Fig. 7. Photograph of a sensorized laparoscopic forceps.

contacting the probed object, while it is relevant at points belonging to the contact area. The phototransistor hence detects a signal roughly proportional to the contact area.

Although the optoelectronic CASR sensor may be somewhat complicate to build in miniaturized scale, it showed superior accuracy in our laboratory experiments. For the purposes of the psychophysical tests to be described shortly, we built a CASR sensor of sufficient accuracy by carefully removing possible artifact causes. In particular, the reflective properties of different objects were equalized by spraying equal colours on their surfaces, and spurious sources of light from outside the sensor were shielded accurately.

Finally, it is noteworthy that sometimes the CASR information can be approximately obtained from processing kinesthetic data according to a specific model of contact. In the minimally invasive surgery tool described in [2], for instance, the mini-invasive forceps is endowed with strain-gauge sensors for measuring the resultant contact force and optoelectronic (PSD) sensors for the apparent displacement impressed to the specimen by the jaws (see fig.7). For each value of the contact force during a palpation experiment, the slope of the force/displacement curve can be used as a rough estimate of the Young's coefficient of elasticity. Using such value in the Hertzian model (7), along with estimates of the curvatures of the undeformed object ($1/R_1$) and jaws ($1/R_2$), a CASR curve estimate is easily obtained. However rough such estimate may appear, its experimental results are acceptable to some extent. In fig.8 the CASR curve computed from kinesthetic data from the forceps is compared with the one obtained with an optoelectronic CASR sensor. The experiment concerned palpation of a spheroidal object (undeformed curvature radius $R_1 \approx 3mm$) realized with a medium-compliance polymeric foam, by means of a flat-jaw forceps ($R_2 = \infty$).

B. CASR display

The role of a CASR display is to replicate the rate at which the contacting area of the probed material spreads on the surface of the remote probing finger. A possible implementation of such behaviour is described in fig.9. The CASR display consists of a set of cylinders of different radii

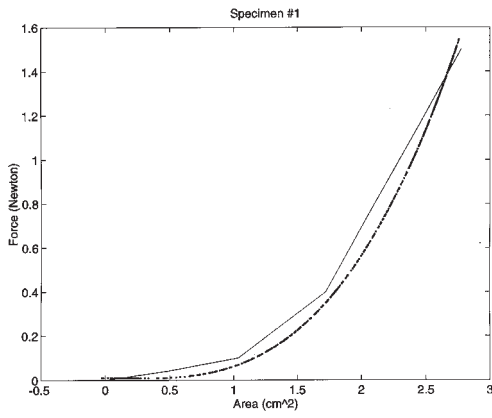


Fig. 8. Comparison between the CASR diagram obtained with an optoelectronic area sensor (solid) and the one computed by Hertzian contact theory on the basis of overall displacement measurements (dotted).

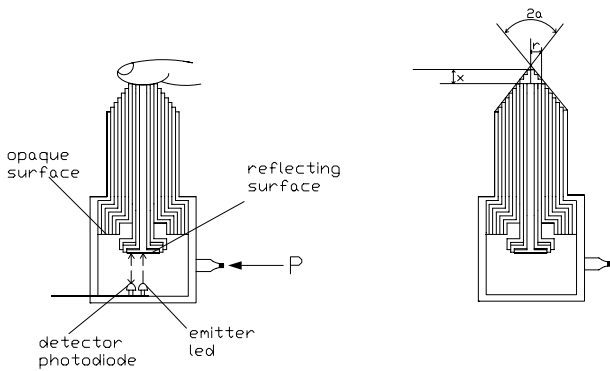


Fig. 9. Description of the CASR display.

in telescopic arrangement. A regulated air pressure acts on one end of the cylinders. The operator finger probes the other end of the display. The length of the cylinders is arranged so that, when no forces are applied by the operator, the active surface of the display is a stepwise approximation of a cone whose total angle at the vertex is $2a$. When the probing finger is lowered by an amount x , an area of contact A approximately evaluated as $A(x) = \pi x^2 \tan^2(a)$ is established. Correspondingly, the force opposed to the finger is $F(x) = PA(x)$, where P is the pressure established in the inner chamber by the external regulator. An optoelectronic sensor placed within the chamber allows measurement of the displacement x , while a servo pneumatic actuator regulates the chamber pressure based on x and on the desired CASR profile to be replicated.

A laboratory prototype of the CASR display, with 10 concentric cylinders, is shown in fig.10, while fig.11 shows the experimental characterization of the CASR effect as measured with several different values of constant pressure P .

As it is apparent from fig.11, the CASR curves of this display at constant pressure are roughly linear. To match typical CASR curves (which are nonlinear, see e.g. fig.8), the haptic display is operated in feedback by controlling pressure in the inner chamber as the display displacement



Fig. 10. The prototype CASR display.

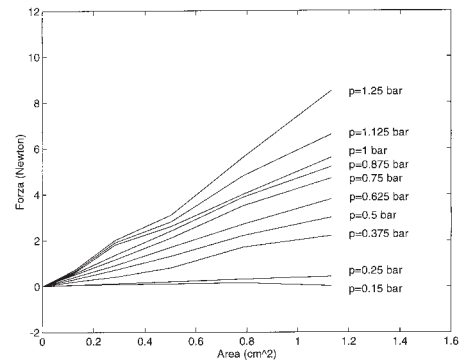


Fig. 11. Force/Area response of the prototype CASR display with constant pressure.

is changed, in such a way as to mimic the CASR function measured on the specimen under exploration. In our implementation, a pneumatic servovalve by Proportion-Air's QB series is employed to this purpose.

IV. EXPERIMENTAL RESULTS

To validate, at least preliminarily, the CASR hypothesis, we devised and executed several psychophysical experiments, which have been conducted in our laboratory with the help of volunteers using the CASR sensing and displaying equipment described above. For comparison purposes, a purely kinesthetic display is used in some experiments. In order to minimize the impact on psychophysical experiments of the different technology and appearance of the kinesthetic display with respect to the CASR haptic display, the former device has been realized by covering the CASR display with a hollow cylinder, whose upper base is flat and rigid (see fig.12).

A. First Experiment: Recognition Rate

The experiment consisted in measuring the capability of 15 volunteers to recognize 5 different items by touching a remote haptic system. Recognition rates using direct exploration, a kinesthetic display, and the CASR paradigm have been compared.



Fig. 12. Appearance of the kinesthetic display used in the experiments.

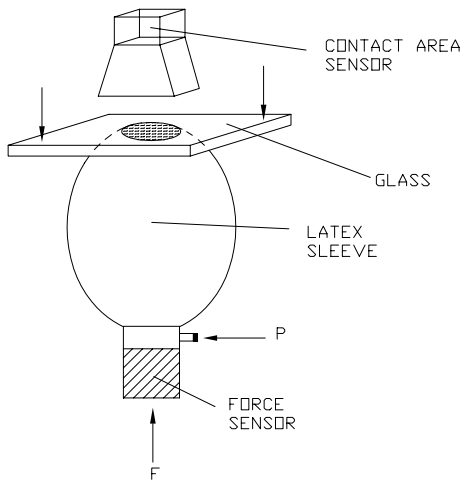


Fig. 13. Variable softness device used in psychophysical experiments.

To do so, we collected 5 sets of data corresponding to the contact of a rigid surface with surfaces of decreasing compliance. In order to keep experimental conditions (superficial texture, colour, thermal properties of the specimens) as constant as possible in experiments with different items, we used a single device with variable softness (see fig.13). The device consists of an inflatable thick Latex sleeve, of which the apparent softness is varied by changing the internal air pressure.

The first phase of the experiment consisted in pressing a flat glass surface against the upper portion of the sleeve for 5 different levels of internal pressure in the sleeve (we will henceforth refer to such different conditions as items #1 through #5). Corresponding to each pressure level, data were gathered concerning the contact force (measured by a load cell shown in fig.13), the displacement, and the area of contact (measured by an optoelectronic sensor through the compressing glass).

In the second phase of the experiment, volunteers wearing surgical latex gloves were allowed to practice in touching the 5 different items. After what was subjectively (by the volunteers) considered a sufficient training, volunteers explored the CASR display described in a previous section,

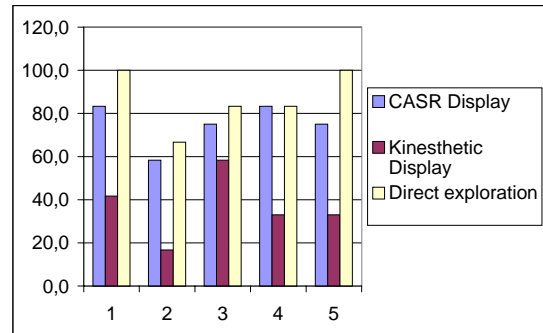


Fig. 14. Percentage of successful recognition of 5 different levels of softness by direct exploration, and by remote exploration using the CASR haptic and the kinesthetic displays.

while the display pressure was controlled in such a way that its contact area would spread, in contact with a rigid surface, at the same rate as one of the sample items. Volunteers were asked to guess which item the display resembled best. This procedure was iterated for all items in random order. No information was given to subjects as to correctness of their guesses. Analogously, volunteers were asked to explore the kinesthetic display, and report on their associations with different items. The display is controlled in this case so as to replicate the apparent displacement/force behaviour of the items. Finally, volunteers were asked to perform recognition of different items by exploration of the original items themselves, presented in random order. Results of the three sets of data concerning correct recognition of different levels of softness are reported in fig.14. Data are referred to 15 subjects, each performing 2 trials on each of the 5 different specimens (for a grand total of 450 trials). Responses by subjects were recorded as either “true” (value 1) or “false” (value 0), and the average response are normalized to 100. It can be observed that the average recognition rate using the CASR information (75%) outperforms pure kinesthesia (37%), and provides results comparable with direct exploration of items (87%).

A statistical study of data significance was done using a two-factor, two replications analysis of variance (see e.g. [16]). Three treatments are considered corresponding to different display types (CASR haptic, kinesthetic, and the original specimen), and five blocks for different levels of pressure. The (null) hypothesis that differences between the first and second treatments are not statistically significant (i.e., that results with the haptic and kinesthetic displays are similar up to experimental accuracy), has a probability of 0.01%, hence can be rejected with p-level 99.99%. The hypothesis that the haptic display provides a perfect perceptual replica of the direct exploration of the specimen, is only significant with p-level 4.8%, hence this can not definitely be considered the case. However, the same hypothesis for the kinesthetic display has much worse p-level $10^{-4}\%$.

B. Second Experiment: Consistency of Perception

An experimental protocol was designed to assess the consistency of users' perception from the haptic and kinesthetic displays. By this protocol, volunteers were required to tune (through instructions given to an assistant) the regulation of the air pressure in the inner chamber of the haptic display, while comparatively exploring one of the specimens described in the previous section, and the display itself, at their will. The assistant himself was blind to what display was being used. Subjects used the same finger for probing the specimen and the display in turns. The tuning procedure was interrupted when the volunteer was subjectively satisfied with the degree of resemblance of the perception from the display and the specimen, and the corresponding pressure level in the display recorded as the perceived optimal tuning parameter (POTP). A completely analogous series of experiments were performed replacing the haptic display with the kinesthetic display. Subjects were aware about which type of display was being used. The experiment was repeated five times by each of the 15 volunteers for the five different specimens and for the two types of display. Experiments with the two displays and the five specimens were executed in mixed order, to equally distribute effects of test fatigue in volunteers.

The mean POTP and its standard deviation for each item and display were subsequently calculated for each subject. These data were averaged over the 15 subjects. The average POTP was then compared with the experimental tuning parameter (ETP) evaluated by experimentally measuring the CASR diagram and choosing the best fit with a curve interpolated from those shown in fig.11. Both the discrepancy between the average POTP obtained with the CASR display and the ETP, and that between the POTP obtained with the kinesthetic display and the ETP, are negligible (no statistically significant advantage of the CASR display over the kinesthetic display results by this criterion). However, averaged standard deviations of POTP differ significantly for the two displays, as reported in fig.15. This indicates that perception of similarity of objects by touch is much more consistent using the CASR display than the kinesthetic display. The analysis of data variance considered in this case two treatments (haptic and kinesthetic displays), five blocks (different pressure levels), and two replications per subject. Results show that the difference between standard deviations of POTP's in the two displays is statistically very significant (the p-level of the alternative hypothesis is $210^{-3}\%$).

C. Third Experiment: Perceptual Thresholds

Important parameters in the psychophysics of perception are absolute and differential thresholds, i.e. the minimum level of intensity of a stimulus capable of evoking a sensation, and the minimum intensity difference between two stimuli that allows the subject to distinguish between them. In the case of haptic discrimination of softness, absolute thresholds are rather difficult to measure, and not as relevant to applications as differential thresholds. We focussed therefore on the assessment of the latter parameter.

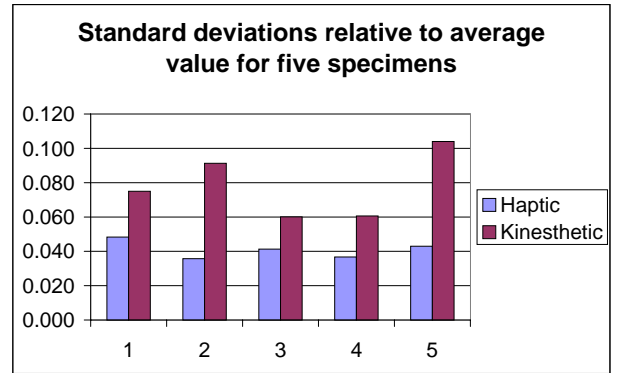


Fig. 15. Standard deviations of perceived optimal tuning parameters (POTP) for the CASR haptic and the kinesthetic displays.

The differential threshold of a perceptual stimulus, or, as it is often called, the *just noticeable difference* (JND), is a figure reflecting the fact that people are usually more sensitive to changes in weak stimuli than they are to similar changes in stronger or more intense stimuli (for instance, one would probably notice a difference in weight between an empty paper cup and one containing a coin, yet probably a difference between a cup containing 100 coins and one containing 101 would not be noticed). The German psychophysicist Weber suggested the simple proportional law $JND = kI$, indicating that the differential threshold increases with increasing intensity I of the stimulus; the constant k is referred to as Weber's constant. Although more recent research indicates that Weber's law should only be regarded as a rough characterization of human sensitivity to changes in stimulation, it approximates reality well in the middle range of stimuli (the JND tends to grow more slowly in the low and high range of reference stimuli). Average values of Weber's constants are available in the psychophysical literature (see e.g. [3]) for most common perceptual channels, among which the two most relevant to our purposes here is for $k = 0.013$ for diffused tactile stimuli, and $k = 0.136$ for punctual tactile stimuli (this numbers indicate the rapid saturation of receptors involved in single-point tactile perception).

In the evaluation of the JND of the CASR haptic display comparatively with the kinesthetic display, the stimulus is represented by the device compliance, and hence the stimulus intensity can be identified with the pressure level in the device. The 15 volunteers were asked to touch the haptic display regulated at a constant reference stimulus, and familiarize with the corresponding compliance by probing the device. Afterwards, the device was regulated at slowly increasing pressures, until the subject, who kept probing the device, would detect a difference in compliance. The difference between the corresponding value of pressure and the reference value was then recorded. All subjects repeated the experiment twice for six different levels of reference

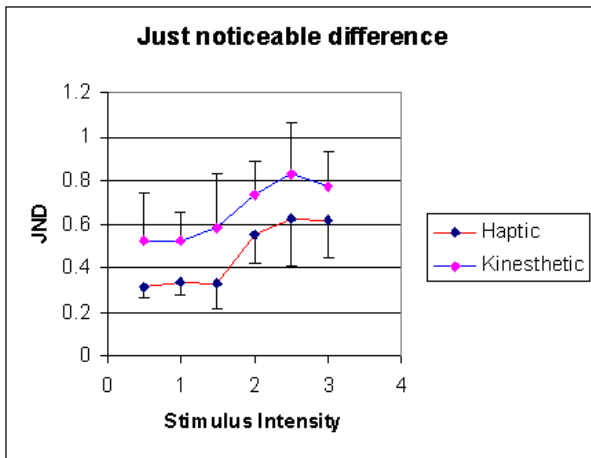


Fig. 16. JND versus the intensity of reference standard stimulus for the CASR display and the purely kinesthetic display. Each data point represents the average of 30 trials (2 trials by 15 subjects). Error bars (segment lengths are equal to half the average of standard deviations for the 15 subjects) are superimposed to data.

pressure, equally spaced in the operating range of the device. The sequence of experiments was randomized. The same procedure was then applied to the kinesthetic device. The mean JND and its standard deviation for each reference stimulus and display type were calculated for each subject, and these data averaged over the 15 subjects. Results are presented in fig.16, along with the corresponding error bars.

Both diagrams are pretty much linear in the medium range, where Weber's constant can be evaluated as ca. $k = 0.09$. Though not as good as diffused cutaneous tactile perception, both displays show a slower growth of JND than single-point stimuli. The average JND of the haptic and kinesthetic displays are 0.46 and 0.66 stimulus units, respectively. The haptic display allows subjects to discriminate differences in compliance 30% more finely than the kinesthetic display. The analysis of variance of these data considered two treatments (haptic and kinesthetic displays), six blocks (different reference stimuli), and two replications per subject, and resulted in a p-level of 99.99% for our conclusion on the superiority of the CASR haptic with respect to the kinesthetic display. Experiments such as that described so far, but adjusting the comparison pressure in descent with respect to the reference level, provided similar results to those shown in fig.16.

D. Fourth experiment: Psychometric function

The psychometric function is another measure of sensory resolution widely used in psychophysical studies. The experiment consists of asking volunteers to compare the apparent compliance of the CASR display in two successive trials. During the first trial, the display is regulated to a standard value S of compliance (i.e. of air pressure in the inner chamber), while during the second a different value X is set. Fifteen volunteers were asked to decide whether X was "harder" than S , and the number of positive an-

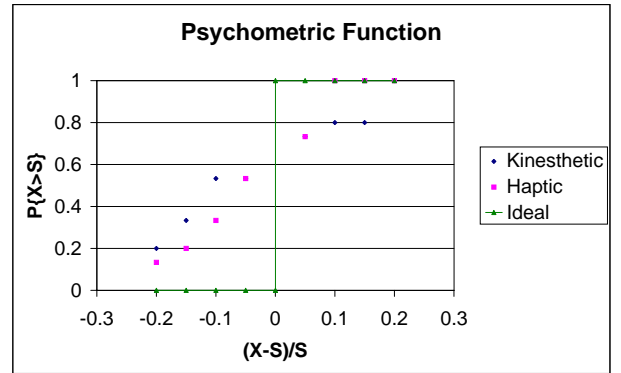


Fig. 17. Psychometric function of the CASR display. The reference stimulus S corresponds to an air pressure of 0.5 bar in the displays, i.e. in the middle of the operating range of the devices. Each data point represents the average of 30 trials (2 trials by 15 subjects).

swers divided by the total number of answers is denoted by $P\{X > S\}$. As X is varied from values lower to values higher than S , the *psychometric function* is obtained as

$$F_S(X) = P\{X > S |_{(S,X)}\}. \quad (8)$$

In the ideal case of an infinitely fine resolution in the sensory channel, the psychometric function would be a step function ($F_S(X) = 0, X < S, F_S(X) = 1, X > S$). A diagram of the psychometric functions obtained with the CASR haptic display and the kinesthetic display is reported in fig.17. The discrepancy between the ideal step function and the experiments can be measured by the sum of the squares of deviations from the ideal, stepwise curve, namely by the figure

$$D = \sum_{i=1}^4 P_i^2 + \sum_{i=5}^8 (1 - P_i)^2$$

It can be observed that the haptic display curve is closer to the ideal behavior ($D = 0.87$) than the kinesthetic display ($D = 0.52$). The analysis of variance (two treatments for CASR haptic and kinesthetic displays, eight blocks for different comparison stimuli, two replications per subject), supports the favorable comparison for the CASR haptic with a confidence p-level of 98%.

E. Fifth Experiment: Perceptual Granularity

An experiment was designed in order to assess how fine a gradation of compliance could be perceived by subjects. Fifteen volunteers were asked preliminarily to practice in probing the display while it was regulated to a value close to its minimum operating level, and afterwards with the display regulated to its maximum level. The interval between these two values was then divided in ten, and subjects were successively presented with the display regulated to these

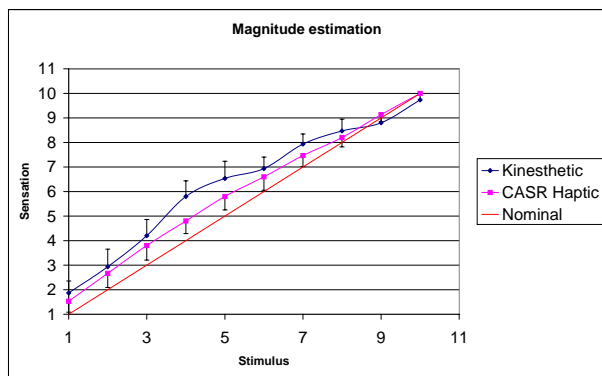


Fig. 18. Average estimates of linearly increasing stimuli with the kinesthetic display differs from the ideal behaviour more than with the CASR-haptic display. Each data point represents the average of 30 trials (2 trials by 15 subjects). Error bars (segment lengths are equal to half the average of standard deviations for the 15 subjects) are superimposed to data.

intermediate levels, twice for each level, in random order. Subjects were asked to rank the perceived compliance in a range of 10, with 1 being the minimum and 10 the maximum levels of which they had previous experience. The average estimate by subjects is presented in fig.18 for both the haptic and kinesthetic display, along with the average over subjects of the standard deviation of each subject's estimates for each level. It can be observed that the granularity of perception is finer for the haptic display: as an overall measure, for instance, the standard deviation of estimates with respect to the ideal linear behaviour is 1.8 for the CASR haptic display, and 3.27 for the kinesthetic display. The analysis of variance of the experiment (two treatments for CASR haptic and kinesthetic displays; ten blocks for different stimulus levels; two replications per subject) provided statistical significance of such comparison of 99.99%.

V. CONCLUSIONS

It has been firmly established in the psychophysical literature that the ability of discriminating softness by touch is intimately related to both kinesthetic and cutaneous tactile information in humans. In replicating touch with remote haptic devices, there are serious technological difficulties to build devices for sensing and displaying fine tactile information. In this paper, we investigated the possibility that a simplified form of tactile data could convey enough information to allow satisfactory discrimination of softness, while allowing practical construction of devices for practical applications. One of these devices is presented in paragraph 4 and has been used to acquire information of different materials necessary to control the haptic display. Results of our psychophysical experiments strongly encourage this hypothesis.

REFERENCES

- [1] G. Ambrosi, A. Bicchi, D. De Rossi, and P. Scilingo: "The Role of Contact Area Spread Rate in Haptic Discrimination of Softness". *Proceedings of the 1999 IEEE International Conference on Robotics and Automation*, pp. 305-310, Detroit, Michigan, may 1999.
- [2] A. Bicchi, G. Canepa, D. De Rossi, P. Iaconi, E. P. Scilingo: "A Sensorized Minimally Invasive Surgery Tool for detecting Tissue Elastic Properties", *Proceedings of the 1996 IEEE International Conference on Robotics and Automation*, pp. 884-888, Minneapolis, Minnesota, April 1996.
- [3] J. C. Falmagne: "Psychophysical Measurement and Theory", in *Handbook of Perception and Human Performance*, K. R. Roff, L. Kaufman, and J. P. Thomas, USA, eds., Wiley Interscience Publ., 1986, Vol. I, chapt. 1, pp 1-66.
- [4] F. J. Clark and K. W. Hork: "Kinesthesia" in *Handbook of Perception and Human Performance*, K. R. Roff, L. Kaufman, and J. P. Thomas, USA, eds., Wiley Interscience Publ., 1986, Vol. I, chapt. 13, p. 1-62.
- [5] M. B. Cohn, L. S. Crawford, J.M.Wendlandt, and S. S. Sastry: "Surgical applications of milli-robots". *Journal of Robotic systems*, 12(6):401-416, June 1995.
- [6] P. Dario and M. Bergamasco: "An advanced robot system for automated diagnostic tasks through palpation," *IEEE Trans. Biomedical Eng.*, 35(2), pp. 118-126, 1988.
- [7] M. B. Cohn, M. Lam, and R. S. Fearing: "Tactile feedback for teleoperators", *Telemanipulator Technology Conf.*, Proc. SPIE vol. 1833, H. Das, ed., 1992.
- [8] P. Green, R. Satava, J. Hill, and I. Simon. Telepresence: "Advanced teleoperator technology for enhanced minimally invasive surgery systems", *Soc. Am. Gastrointestinal Surgeons*, April 1992.
- [9] R. D. Howe, W. J. Peine, D. A. Kontarinis, and J. S. Son: "Remote palpation technology", *IEEE Eng in Medicine and Biology Magazine*, 14(3):318-323,1995.
- [10] R. S. Johansson and G. Westling: "Roles of glabrous skin receptors and sensorimotor memory in automatic control of precision grip when lifting rougher or more slippery objects", *Experimental Brain research*, 56, pp. 550-564, 1984.
- [11] K. L. Johnson: "Contact mechanics", chapter 4, Cambridge University Press 1985.
- [12] S. J. Lederman and R. L. Klatzky: "Sensing and displaying spatially distributed fingertip forces in haptic interfaces for teleoperator and virtual environment studies", Presence, 1998 (in press).
- [13] N. Hogan: "Impedance Control: an Approach to Manipulation", *ASME J. Dynamic Systems, Measurement, and Control*, vol. 107, pp. 1-7 and 8-16, 1985.
- [14] J. M. Loomis and S. J. Lederman: "Tactual perception", *Handbook of Perception and Human Performance*, Wiley, 1986, Vol. II, chapt. 31, p. 1-41.
- [15] T. H. Massie and J. K. Salisbury. "The phantom interface: A device for probing virtual objects", *ASME Winter Annual Meeting, Symposium on Hatic Interfaces for a virtual environment and teleoperator systems*, November 1994.
- [16] D. C. Montgomery: "Design and analysis of experiments", J. Wiley & Sons, 1997.
- [17] R. Pallás-Areny and J. G. Webster: "Sensors and signal conditioning", Wiley, 1991.
- [18] D. T. V. Pawluk, W. J. Peine, P. S. Wellmann, and R. Howe: "Simulating soft tissue with a tactile shape display", in *Advances in Bioengineering*, B. Simon, ed., ASME BED-Vol.36
- [19] E.P. Scilingo, D. DeRossi, A. Bicchi, P. Iacone: "Haptic display for replication of rheological behaviour of surgical tissues: modelling, control, and experiments", *Proc. Sixth Annual Symp. on Haptic Interfaces for Virtual Environments and Teleoperator Systems*, Dallas, November 1997.
- [20] W. Sjoerdsma, J.L. Herder, M.J. Horwrad, A. Jansen, J.J.G. Bannenberg, and C.A. Grimbergen: "Force transmission of laparoscopic instruments", *Min. Invas. Ther. & Allied Technol.*, vol. 6, pp.274-278, 1997.
- [21] M. A. Srinivasan and R. H. LaMotte, "Tactile Discrimination of Softness", *Journal of Neurophysiology*, Vol. 73, No. 1, pp. 88-101, Jan 1995.
- [22] T. Yoshikawa, Y. Yokokohji, T. Matsumoto, X. Zheng: "Display of Feel for the Manipulation of Virtual Objects", *ASME J. Dyn. Systems, Measurement, and Control*, Vol. 117, no. 4, pp.554-558, 1995.